

Hubbard models for materials with nonlocal Coulomb interactions: graphene, silicene and benzene

M. Schüler,^{1,2,*} M. Rösner,^{1,2} T. O. Wehling,^{1,2} A. I. Lichtenstein,³ and M. I. Katsnelson⁴

¹*Institut für Theoretische Physik, Universität Bremen, Otto-Hahn-Allee 1, 28359 Bremen, Germany*

²*Bremen Center for Computational Materials Science,*

Universität Bremen, Am Fallturm 1a, 28359 Bremen, Germany

³*Institut für Theoretische Physik, Universität Hamburg, Jungiusstraße 9, D-20355 Hamburg, Germany*

⁴*Radboud University of Nijmegen, Institute for Molecules and Materials,*

Heijendaalseweg 135, 6525 AJ Nijmegen, The Netherlands

(Dated: February 11, 2019)

We report on a method to approximate a generalized Hubbard model with nonlocal Coulomb interactions by an effective Hubbard model with on-site interactions U^* only. The effective model is defined by the Peierls-Feynman-Bogoliubov variational principle. We find that the local part of the interaction U is reduced according to $U^* = U - \bar{V}$, where \bar{V} is an average of nonlocal Coulomb interactions weighted according to derivatives of nonlocal charge correlation functions from the effective model. For the examples of graphene, silicene and benzene we show that the nonlocal Coulomb interaction can decrease the effective local interaction by more than a factor of 2.

PACS numbers: 72.80.Rj; 73.20.Hb; 73.61.Wp

Low dimensional *sp*-electron systems like graphene [1–3], systems of adatoms on semiconductor surfaces, such as Si(111):X with X=C, Si, Sn, Pb [4], Bechgaard salts or aromatic molecules [5, 6] feature simultaneously strong local and nonlocal Coulomb interactions. In graphene for instance, the on-site interactions $U/t \sim 3.3$, the nearest neighbor Coulomb repulsion $V/t \sim 2$ as well as further sizable nonlocal Coulomb terms exceed the nearest neighbor hopping $t = 2.8$ eV [1]. Considering on-site interactions $U/t \sim 3.3$ alone would put graphene close to the boundary of a gapped spin-liquid [7], which could be even crossed by applying strain on the order of a few percent [1]. It is currently unclear, whether [8] or not [9] nonlocal Coulomb interaction stabilize the semimetallic Dirac phase in graphene. To rephrase the problem: It is unclear which Hubbard model with strictly local interactions would yield the best approximation to the ground state of graphene. To judge the stability of the Dirac electron phase in graphene but also to understand Mott transitions on surfaces like Si:X (111), a quantitative well defined link from models with local and nonlocal Coulomb interactions to those with purely local interactions is desirable.

In this letter, we present a method to map a generalized Hubbard model with nonlocal Coulomb interactions onto an effective Hubbard model with on-site interactions U^* only. Using the examples of graphene, silicene and benzene we show that nonlocal terms can significantly reduce the effective on-site interaction. For graphene, this reduction is $U^*/U \approx 0.45$. Thus, nonlocal Coulomb interactions are found to stabilize the Dirac electron phase against spin-liquid and antiferromagnetic instabilities. We begin with a description of the theoretical framework and afterwards present its application to graphene, silicene and benzene.

The starting point is the extended Hubbard model

$$H = - \sum_{i,j,\sigma} t_{ij} c_{i\sigma}^\dagger c_{j\sigma} + U \sum_i n_{i\uparrow} n_{i\downarrow} + \frac{1}{2} \sum_{\substack{i \neq j \\ \sigma, \sigma'}} V_{ij} n_{i\sigma} n_{j\sigma'}, \quad (1)$$

where t_{ij} are the hopping matrix elements and U and V_{ij} are the local and nonlocal Coulomb matrix elements, respectively. The goal is to map the Hamiltonian (1) onto the effective model

$$H^* = - \sum_{i,j,\sigma} t_{ij} c_{i\sigma}^\dagger c_{j\sigma} + U^* \sum_i n_{i\uparrow} n_{i\downarrow}. \quad (2)$$

The effective on-site interaction U^* shall be chosen such that the canonical density operator $\rho^* = 1/Z^* e^{-\beta H^*}$ of the auxiliary system, where $Z^* = \text{Tr} \{e^{-\beta H^*}\}$ is the partition function, approximates the exact density operator ρ derived from H as close as possible. This requirement leads to the Peierls-Feynman-Bogoliubov variational principle [10–12] for the functional

$$\tilde{\Phi}[\rho^*] = \Phi^* + \langle H - H^* \rangle^*, \quad (3)$$

where $\Phi^* = -\frac{1}{\beta} \ln Z^*$ is the free energy of the auxiliary system. $\langle \dots \rangle^*$ denotes thermodynamic expectation values with respect to the auxiliary system: $\langle H - H^* \rangle^* = \text{Tr} \rho^* (H - H^*)$. In the case of $\rho^* = \rho$ the functional $\tilde{\Phi}[\rho^*]$ becomes minimal and coincides with the free energy. The optimal U^* is thus obtained for minimal $\tilde{\Phi}[\rho^*] = \tilde{\Phi}[U^*]$:

$$\partial_{U^*} \tilde{\Phi}[U^*] = 0. \quad (4)$$

By evaluating Eq. (4) one finds

$$U^* = U + \frac{1}{2} \sum_{\substack{i \neq j \\ \sigma, \sigma'}} V_{ij} \frac{\partial_{U^*} \langle n_{i\sigma} n_{j\sigma'} \rangle^*}{\sum_l \partial_{U^*} \langle n_{l\uparrow} n_{l\downarrow} \rangle^*}. \quad (5)$$

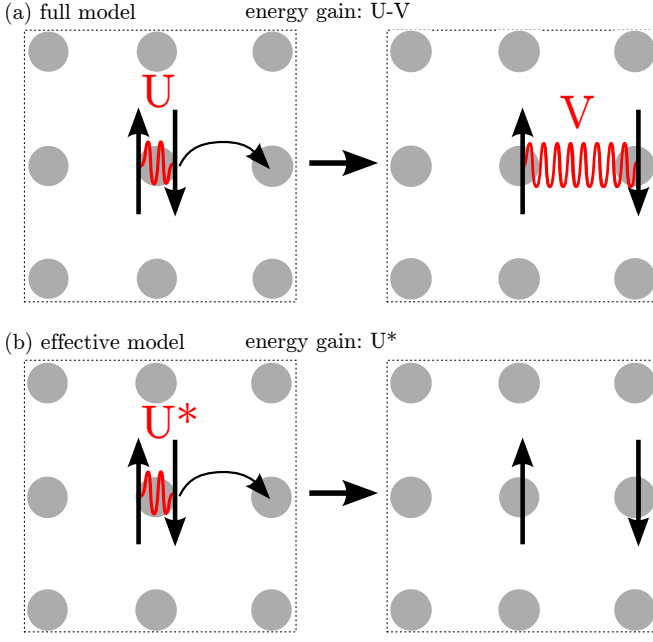


Figure 1. (Color online) Illustration of physical process underlying Eq. (5). Wavy lines illustrate Coulomb interactions. (a) An electron in the extended Hubbard model hopping from a doubly occupied place to an empty place, gaining an energy $U - V$. (b) The same situation in the effective model leads to an energy gain of U^* .

This rule presents a central result of this letter and has an intuitive physical interpretation (Fig. 1): Increasing the on-site term U^* reduces the double occupancy $\langle n_{i\uparrow}n_{i\downarrow} \rangle^*$ and pushes away electrons approaching an already occupied site $i = 0$ to neighboring sites. In case of purely local Coulomb interactions there is a Coulomb energy gain of U^* upon suppressing the double occupancy (Fig. 1b). When there are, however, nonlocal Coulomb interactions with surrounding lattice sites j , the displaced electrons raise the energy of the system by terms proportional to V_{0j} . For a simple case of two electrons on one site this process is depicted in Fig. 1a. In this case, it is obvious that the Coulomb energy gain due to the electron displacement in the full and the auxiliary model become energetically equivalent for $U^* = U - V$. In general, this energy gain depends both on to which sites the charge density is displaced due to the local Coulomb interaction and on how strong the nonlocal Coulomb terms are.

For a translationally invariant system, the local part of the interaction U is reduced according to $U^* = U - \bar{V}$, where

$$\bar{V} = - \sum_{j \neq 0} V_{0j} \frac{\partial_{U^*} \langle n_{0\uparrow} n_{j\sigma'} \rangle^*}{\partial_{U^*} \langle n_{0\uparrow} n_{0\downarrow} \rangle^*}. \quad (6)$$

The conservation of the total electron number N leads to the sum rules $\sum_{j\sigma} \langle n_{0\uparrow} n_{j\sigma} \rangle^* = N/2$ and

$\partial_{U^*} \langle n_{0\uparrow} n_{0\downarrow} \rangle^* = - \sum_{j \neq 0, \sigma} \partial_{U^*} \langle n_{0\uparrow} n_{j\sigma} \rangle^*$. Thus, \bar{V} is a weighted average of the nonlocal Coulomb interactions. It is reasonable that \bar{V} is positive (repulsive) in most situations that correspond to real materials. Then the nonlocal Coulomb interaction reduces the effective on-site interaction and therefore stabilizes the Fermi sea against transitions e.g. to a Mott insulator. Nevertheless, models with negative \bar{V} can easily be constructed and it remains to be seen which real materials lead to negative (attractive) \bar{V} .

Under the assumption that an increasing U^* displaces electrons only to next neighbors, we find $\partial_{U^*} \langle n_{0\uparrow} n_{0\downarrow} \rangle^* = -N_n \partial_{U^*} \sum_{\sigma} \langle n_{0\uparrow} n_{1\sigma'} \rangle^*$, where N_n is the coordination number. Equation. (5) then yields

$$U^* = U - V_{01}. \quad (7)$$

This result is appealingly simple and gives an estimate for the effective Coulomb interaction, without the need of numerical calculations. It follows, however, from a severe approximation. The following numerical calculations show that Eq. (7) nevertheless leads to values close to the exact ones (shown in table I).

When the approximation that electrons are only displaced to next neighbors is dropped, the derivatives of the correlation functions have to be calculated explicitly. This can be done approximately within the dynamical mean field theory [13] and diagrammatic extensions like the Dual-Fermion approach [14]. In certain cases also numerically exact calculations of the nonlocal charge correlation functions for instance by means of determinant quantum Monte Carlo (DQMC [15]) or density-matrix renormalization group methods (e.g. [16]) are possible.

In the following, we consider graphene and benzene, where the computational effort of the DQMC method is manageable for sufficiently small lattice sizes. Therefore, we used the DQMC implementation “QUANTUM Electron Simulation Toolbox” (QUEST 1.3.0 [17]) on a super cell to obtain the charge correlation functions that enter Eq. (5). For small systems a different implementation [18] was used to verify the results of the QUEST package. The Hubbard model with less than 8-9 sites can also be solved by exact diagonalization (ED). In this case a comparison with data obtained with DQMC shows excellent agreement. To overcome the statistical noise from the DQMC calculations, we fit the correlation functions with polynomials of rank 4 in U^* and evaluate the derivative analytically. To evaluate Eq. (5) in a numerically stable way for extended systems like graphene, a cutoff r_c is introduced. All derivatives of the correlation functions for which the distance between site i and j is bigger than r_c are neglected. A reasonable convergence is found for a cutoff at the fourth next neighbor.

To calculate U^* for realistic systems, we introduce values for the Coulomb interactions in the original model defined by Eq. (1). For graphene and silicene these values are calculated with the constrained random phase

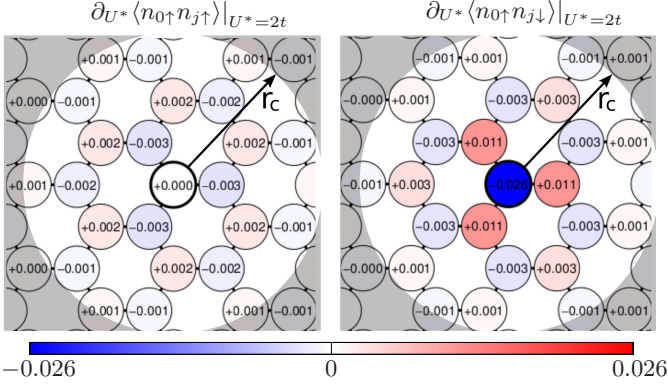


Figure 2. (Color online) Derivatives of the correlation functions $\langle n_{0\uparrow} n_{j\sigma} \rangle$ with respect to U^* for graphene (16x16 unit cells) calculated with DQMC for inverse temperature $\beta = 9t$ and $U = 2t$. Each circle corresponds to one carbon atom. The shaded area depicts the region of nearly vanishing derivatives. The cutoff radius is r_c . The thick drawn circles indicate the lattice site with index $i = 0$.

approximation (cRPA) [19] like in [1]. For benzene, we use values from [20], which are obtained by fitting U and t to experimental spectra and calculating V_{ij} by Ohno interpolation [21]. For all systems the values of the initial Coulomb interactions are given in table I.

For a honeycomb lattice at half filling the U^* -derivatives of the correlation functions $\partial_{U^*} \langle n_{0\uparrow} n_{j\sigma'} \rangle^*$ for $U^* = 2t$ are shown in Fig. 2. In this particular case, $\partial_{U^*} \langle n_{0\uparrow} n_{j\sigma'} \rangle^*$ changes sign with both sublattice and spin indices. Generally, $|\partial_{U^*} \langle n_{0\uparrow} n_{j\downarrow} \rangle^*|$ with opposite spins (right panel) exceeds the equal spin case $|\partial_{U^*} \langle n_{0\uparrow} n_{j\uparrow} \rangle^*|$ (left panel). The derivatives decrease with the distance between the sites $i = 0$ (thick drawn circles in the middle) and j . According to Eq. (6), the derivatives of the correlation functions are the weight of the average of the V_{0j} to calculate U^* . Thus, the oscillating behavior of the correlation function with respect to the sublattice as well as the spin direction speeds up the convergence of Eq. (5) with the cutoff r_c .

An exemplary result of the evaluation of Eq. (5) for different r_c is shown in Fig. 3. (See [22] for computational details.) The error bars are determined by the statistical errors of the DQMC calculations. As could be already expected from the $\partial_{U^*} \langle n_{0\uparrow} n_{j\sigma'} \rangle^*$ -terms depicted in Fig. 2, the nearest neighbor Coulomb interaction has the strongest impact on the renormalization of the on-site term U^* . Thus, the approximation of neglecting all non nearest neighbors terms is quite reasonable, here. Contributions from the same sublattice as the site $i = 0$ tend to increase U^* and those from the other sublattice decrease U^* . It is obviously sufficient to introduce the cutoff after the fourth nearest neighbors.

The resulting values of the effective local Coulomb interaction U^* for graphene, silicene and benzene are sum-

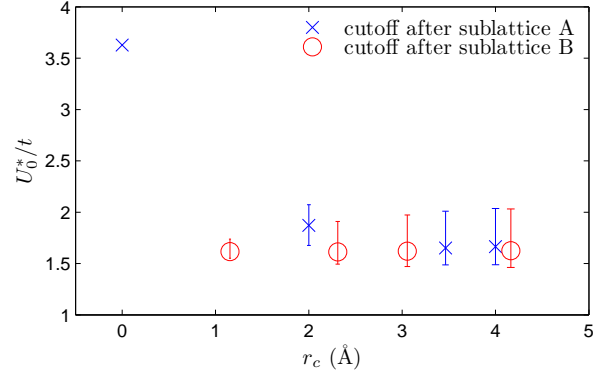


Figure 3. (Color online) Effective Coulomb interaction U^* for graphene against the position of the cutoff used to evaluate Eq. (5).

marized in table I. The local Coulomb interaction is decreased by a factor of larger than two in all cases. For both, graphene and silicene the renormalized on-site interactions $U^*/t = 1.6 \pm 0.2$ and $U^*/t = 2.0 \pm 0.3$ are far away from the transition to a gapped spin liquid at $U^*/t = 3.5$ [7]. The Dirac semimetal phase is thus stabilized by the nonlocal Coulomb interactions.

We obtain the strongest renormalization of the on-site interaction for benzene. This is mostly due to the different ratio between local and nonlocal Coulomb interactions in benzene, $V_{01}/U = 0.72$, as compared to $V_{01}/U = 0.56$ for graphene [23] or $V_{01}/U = 0.55$ for silicene.

Table I. First three rows: Coulomb matrix elements obtained with cRPA ($t_{\text{graphene}} = 2.80$ eV, $t_{\text{silicene}} = 1.14$ eV, $t_{\text{benzene}} = 2.54$ eV). Last three rows: Effective local Coulomb matrix elements with and without the approximation that electrons are only displaced to next neighbors and the factor by which the local Coulomb interaction is decreased.

	Graphene	Silicene	Benzene
U/t	3.63	4.19	3.96
$(V_{01}, V_{02})/t$	2.03, 1.45	2.31, 1.72	2.83, 2.01
$(V_{03}, V_{04})/t$	1.32, 1.14	1.55, 1.42	1.80
U^*/t	1.6 ± 0.2	2.0 ± 0.3	1.2
$(U - V_{01})/t$	1.6	1.9	1.1
U^*/U	0.45 ± 0.05	0.46 ± 0.05	0.3

Naturally, the question arises how accurate the effective model reflects the physical properties of the original model. The phase diagram of the extended Hubbard model on the honeycomb lattice includes an anti-ferromagnetic (AF), a semimetal (SM) and a charge density wave (CDW) phase [24], while the Hubbard model with strictly local interactions only features the first two phases. If the parameters of the extended model are clearly inside the AF or the SM phase, the effective model will likely approximate the physical properties of the orig-

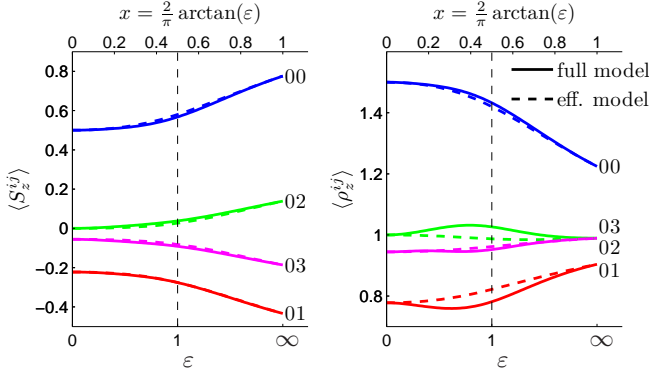


Figure 4. (Color online) Correlation as functions of the screening for the extended Hubbard model (full model, continuous lines) and the effective Hubbard model (broken lines) for benzene. The left panel shows the spin correlation function $\langle S_z^{ij} \rangle$ and the right panel shows the density correlation function $\langle \rho_z^{ij} \rangle$. $\langle S_z^{01} \rangle$ is virtually the same for the effective and full model. The parameters for the full model are $U = 10.06$ eV, $t_{\text{full}} = 2.539$ eV and the non local Coulomb interaction $V(\epsilon)$ is calculated by Eq. (8). The local interaction for the effective model $U^*(\epsilon)$ is calculated by (5), while $t_{\text{eff.}} = t_{\text{full.}}$

inal model quite well. If the full system is, however, close to the CDW phase, a failure of the auxiliary model to provide a physically correct description of the original situation can be expected.

We illustrate this expectation with the example of modified benzene. In this modified model, the nonlocal Coulomb interaction

$$V_{ij}(\epsilon) = \frac{U}{\sqrt{1 + (\alpha \epsilon r_{ij})^2}} \quad (8)$$

with $\alpha = U/e^2$ is tuned by an additional variable screening ϵ ranging from 0 to ∞ . $\epsilon = \infty$ corresponds to purely local interactions and $\epsilon = 0$ ultimately nonlocal interactions with matrix elements not decaying with distance between the involved electrons. A comparison of the spin $\langle S_z^{ij} \rangle = \langle (n_{i\uparrow} - n_{i\downarrow})(n_{j\uparrow} - n_{j\downarrow}) \rangle$ and the density correlation functions $\langle \rho_z^{ij} \rangle = \langle (n_{i\uparrow} + n_{i\downarrow})(n_{j\uparrow} + n_{j\downarrow}) \rangle$ for the extended and the auxiliary local Hubbard model are shown in Fig. 4. The correlation functions shown here have been calculated by exact diagonalization for, both, the full and the effective model. For $\epsilon = 0$ and $\epsilon \rightarrow \infty$ (non-interacting limit) the correlation functions of the effective and full model coincide as they should. CDW physics would manifest in $\langle \rho_z^{ij} \rangle$ and here we find indeed some differences of $\langle \rho_z^{ij} \rangle$ for the effective and the auxiliary model for intermediate screening ($\epsilon \sim 1$). However, nearly no deviation of $\langle S_z^{ij} \rangle$ between the full and effective model is found. We thus expect that transitions into phases like an AF insulator (or a Mott insulator) will be very well described by the effective model.

In conclusion, a systematic map from a generalized Hubbard model with nonlocal Coulomb interactions to

an effective Hubbard model with strictly local Coulomb interactions U^* is derived. The physical properties of the effective model reflect the original system nicely, especially regarding spin related properties. We find that the nonlocal Coulomb interactions can significantly renormalize the effective on-site interaction U^* as compared to the original local U . In the cases of graphene and silicene our calculations yield $U^*/U < 0.5$. Thus, the nonlocal Coulomb interactions stabilize the Dirac semimetallic phases in these materials against transitions to a gapped spin liquid or an antiferromagnetic insulator. In defective graphene or at edges local Coulomb interactions can lead to the formation of magnetic moments [3, 25, 26]. When describing these situations in terms of the Hubbard model, the value of $U^* = 1.6t$ obtained here should be used. For all materials studied, here, $U^* \approx U - V_{01}$, Eq. (7), yields a qualitatively correct estimate of the effective local interactions without the need for numerical calculations. We therefore speculate that nonlocal Coulomb interactions will significantly weaken local correlation effects in *sp*-electron materials, in general.

Acknowledgements. The authors thank F. Assaad for providing his DQMC code and D. Mourad for helpful discussions. Financial support from DFG via SPP 1459 and FOR 1346 are acknowledged. MIK acknowledges a support from FOM (Netherlands).

* mschueler@itp.uni-bremen.de

- [1] T. O. Wehling, E. Şaşıoğlu, C. Friedrich, A. I. Lichtenstein, M. I. Katsnelson, and S. Blügel, *Physical Review Letters* **106**, 236805 (2011)
- [2] V. N. Kotov, B. Uchoa, V. M. Pereira, F. Guinea, and A. H. Castro Neto, *Rev. Mod. Phys.* **84**, 1067 (2012)
- [3] M. I. Katsnelson, *Graphene: Carbon in Two Dimensions* (Cambridge University Press, 2012)
- [4] P. Hansmann, T. Ayrar, L. Vaugier, P. Werner, and S. Biermann(2013), arXiv:1301.4325
- [5] R. Pariser and R. G. Parr, *The Journal of Chemical Physics* **21**, 767 (1953)
- [6] J. A. Pople, *Proc. Phys. Soc. A* **68**, 81 (1955)
- [7] Z. Y. Meng, T. C. Lang, S. Wessel, F. F. Assaad, and A. Muramatsu, *Nature* **464**, 847 (2010)
- [8] J. Jung and A. H. MacDonald, *Phys. Rev. B* **84**, 085446 (2011)
- [9] C. Honerkamp, *Phys. Rev. Lett.* **100**, 146404 (2008)
- [10] R. E. Peierls, *Phys. Rev.* **54**, 918 (1938)
- [11] N. N. Bogoliubov., *Dokl. Akad. Nauk SSSR* **119**, 244 (1958)
- [12] R. P. Feynman, *Statistical Mechanics* (Benjamin, Reading Mass., 1972)
- [13] A. Georges, G. Kotliar, W. Krauth, and M. J. Rozenberg, *Reviews of Modern Physics* **68**, 13 (1996)
- [14] A. N. Rubtsov, M. I. Katsnelson, and A. I. Lichtenstein, *Physical Review B* **77**, 033101 (2008)
- [15] R. Blankenbecler, D. J. Scalapino, and R. L. Sugar, *Physical Review D* **24**, 2278 (1981)
- [16] R. M. Noack, S. R. White, and D. J. Scalapino,

- Physical Review Letters **73**, 882 (1994)
- [17] Downloadable at <http://quest.ucdavis.edu/>
 - [18] We used the DQMC implementation by DQMC Fakhri F. Assaad from the University of Würzburg
 - [19] F. Aryasetiawan, M. Imada, A. Georges, G. Kotliar, S. Biermann, and A. I. Lichtenstein, Physical Review B **70**, 195104 (2004)
 - [20] R. J. Bursill, C. Castleton, and W. Barford, Chemical Physics Letters **294**, 305 (1998)
 - [21] K. Ohno, Theoretica chimica acta **2**, 219 (1964)
 - [22] DQMC calculations with 16x16 unit cells, $\beta = 9t$, $\Delta\tau = 0.05$, 3000 measurement sweeps and 48 U^*/t steps from 0.2 in steps of $\Delta U^*/t = 0.1$
 - [23] A comparison with a graphene result for 8x8 unit cells, which yields the same ratio U/U^* , rules out finite size effects of the DQMC calculations.
 - [24] I. F. Herbut, Physical Review Letters **97**, 146401 (2006)
 - [25] M. P. López-Sancho, F. de Juan, and M. A. H. Vozmediano, Physical Review B **79**, 075413 (2009)
 - [26] O. V. Yazyev, Reports on Progress in Physics **73**, 056501 (2010)